HHS Public Access

Author manuscript

Oncogene. Author manuscript; available in PMC 2011 January 01.

Published in final edited form as:

Oncogene. 2010 July 1; 29(26): 3781–3792. doi:10.1038/onc.2010.134.

A TRANSCRIPTIONAL CROSS–TALK BETWEEN RhoA AND c–Myc INHIBITS THE RhoA/Rock–DEPENDENT CYTOSKELETON

Vincent Sauzeau[1,2,†], **Inmaculada M. Berenjeno**[1,2,†,§], **Carmen Citterio**[1,2], and **Xosé R. Bustelo**[1,2,*]

[1]Centro de Investigación del Cáncer, CSIC–University of Salamanca, Campus Unamuno, E37007 Salamanca, Spain

[2]Instituto de Biología Molecular y Celular del Cáncer (IBMCC), CSIC–University of Salamanca, Campus Unamuno, E37007 Salamanca, Spain

Abstract

The GTPase RhoA participates in a number of cellular processes, including cytoskeletal organization, mitogenesis and tumorigenesis. We have previously shown that the transforming activity of an oncogenic version of RhoA (Q63L mutant) was highly dependent on the transcriptional factor c–Myc. In contrast to these positive effects in the RhoA route, we show here that c–Myc affects negatively the F–actin cytoskeleton induced by $RhoA^{Q63L}$ and its downstream effector, the serine/threonine kinase Rock. This effect entails the activation of a transcriptional program that requires synergistic interactions with RhoA–derived signals and that includes the upregulation of the GTPase Cdc42 and its downstream element Pak1 as well as the repression of specific integrin subunits. The negative effects of c–Myc in the F–actin cytoskeleton are eliminated by the establishment of cell–to–cell contacts, an effect associated with the rescue of Pak1 and integrin levels at the post–transcriptional and transcriptional levels, respectively. These results reveal the presence of a hitherto unknown signaling feed–back loop between *RhoA* and *c–Myc* oncogenes that can contribute to maintain fluid cytoskeletal dynamics in cancer cells.

Keywords

RhoA; c–Myc; Rho/Rac GTPases; Pak; integrin; stress fibers; focal adhesions; F–actin; microarray; gene expression; transcription

INTRODUCTION

RhoA is a GTP–binding protein that belongs to the Rho/Rac GTPase subfamily (Bustelo et al., 2007; Etienne–Manneville & Hall, 2002; Jaffe & Hall, 2005). This protein plays critical roles in general cell functions such as F–actin cytoskeletal dynamics, mitogenesis and cell

*To whom correspondence should be addressed: xbustelo@usal.es / **Phone:** +34–923294802 / **Fax:** +34–923294743.

†These two authors contributed equally to this work.

§Present address: Institute of Cancer, Barts and the London School of Medicine and Dentistry, Charterhouse Square, London, EC1M 6BQ, United Kingdom

survival as well as in cell type–specific biological processes that include, among others, arterial contractility, axogenesis and phagocytosis (Bustelo et al., 2007; Etienne–Manneville & Hall, 2002; Jaffe & Hall, 2005). To carry out those functions, RhoA engages a wide collection of downstream effectors that work as protein kinases, lipid–related enzymes or scaffolding proteins (Bustelo et al., 2007; Jaffe & Hall, 2005). Among those effectors, RockI and RockII are perhaps the best characterized at the structural, regulatory, and biological levels (Mueller et al., 2005; Riento & Ridley, 2003). These serine/threonine kinases mediate the formation of stress fibers and focal adhesions, thereby participating in cell–to–cell and cell–to–substratum adhesion, cell migration and invasiveness, neurite retraction and phagocytosis (Mueller et al., 2005; Riento & Ridley, 2003).

In addition to the canonical regulation of RhoA by guanosine nucleotide exchange factors (GEFs), GTPase activating proteins (GAPs), and Rho GDP dissociation inhibitors (RhoGDIs) which is common to most Rho/Rac proteins (Bos et al., 2007; Dransart et al., 2005; Olofsson, 1999), the signaling output of RhoA can be controlled by unique mechanisms. Those include its proteosomal degradation via the ubiquitin ligase Smurf1 (Sahai et al., 2007; Wang et al., 2006; Wang et al., 2003), the inactivation of Rock proteins by the binding to either the cell cycle inhibitor $p21^{WAF}$ (Lee & Helfman, 2004) or RhoE, Gem and Rad GTPases (Hatzoglou et al., 2007; Riento et al., 2003; Ward et al., 2002), and the stimulation of Rock activity by dephosphorylation by the Shp2 phosphatase (Lee & Chang, 2008). The signal output from the RhoA route can be also influenced by more distal, transcriptional–based mechanisms. Hence, it has been shown that the tumor suppressor p53 activates *RhoE* gene transcription, leading to the inhibition of Rock–dependent effects (Ongusaha et al., 2006). Proteomic experiments have revealed that c–Myc can regulate the activity of RhoA–dependent routes by lowering the levels of RhoA, Cdc42, Rock and a subset of cytoskeletal–related proteins (Shiio et al., 2002). It is important to note that these regulatory influences are usually bidirectional, a property that facilitates the establishment of feed–back loops that can provide further plasticity to GTPase–regulated processes. Consistent with this view, it has been shown that RhoA and Cdc42 can stimulate and repress c–Myc (Berenjeno et al., 2007; Watnick et al., 2003) and p53 (Park et al., 2009), respectively. In this work, we present evidence indicating that there exists another cross–talk between c–Myc and RhoA that contributes to the dowmodulation of the RhoA/Rock cytoskeleton in mouse fibroblasts. Interestingly, this transcriptional program is inhibited by the establishment of cell–to–cell contacts both at the transcriptional and posttranslational level, a property that gives further flexibility to the modulation of F–actin cytoskeletal dynamics in vivo.

RESULTS

Overexpression of c–Myc leads to the disruption of $RhoA^{Q63L}$–induced stress fibers and focal adhesions

During a previous study (Berenjeno et al., 2007), we generated a number of NIH3T3 cell derivatives expressing $RhoA^{Q63L}$, c–Myc, $RhoA^{Q63L}$ plus c–Myc, and $RhoA^{Q63L}$ plus either a c–Myc dominant negative mutant (MadMyc) or a c–*Myc*–specific short hairpin RNA (shRNA). Using those cell lines, we demonstrated that c–Myc was important for both

the loss of cell contact inhibition and cell transformation induced by the *RhoA*^{Q63L} oncogene in fibroblasts (Berenjeno et al., 2007). To further characterize the effect of the c–Myc network in the transformation mediated by this GTPase, we decided to check the status of the F–actin cytoskeleton in these cells using microscopy techniques. As previously described (Berenjeno et al., 2007), we observed that RhoA^{Q63L}–transformed cells contained robust stress fibers when compared with the parental cell line (Fig. 1A). However, this cytoskeletal phenotype was lost in cell lines co–expressing RhoA^{Q63L} and c–Myc (Fig. 1A and data not shown) but not in those co–expressing RhoA^{Q63L} with either MadMyc (Fig. 1A) or a c–*Myc* specific shRNA (Fig. 1A). The comparison of parental and c–Myc expressing NIH3T3 cells indicated that the overexpression of c–Myc alone also induced the disruption of stress fibers (Fig. 1A). This effect, however, was less conspicuous than that found in the case of RhoA^{Q63L}–transformed cells because of the lower levels of stress fibers present in the parental NIH3T3 cells (Fig. 1A). In agreement with the confocal microscopy data, we found using flow cytometry experiments that cell lines co–expressing RhoA^{Q63L} and c–Myc had lower F–actin levels than those expressing exclusively RhoA^{Q63L} (Fig. 1B,C). These analyses also indicated that the co–expression of MadMyc further elevated the total levels of F–actin induced by RhoA^{Q63L} (Fig. 1B,C), suggesting that the increased levels of endogenous c–Myc protein induced by RhoA^{Q63L} also contribute to tuning down the RhoA^{Q63L}–dependent F–actin cytoskeleton in fibroblasts. Western blot experiments indicated that negative effect of c–Myc in the F–actin cytoskeleton was not due to alterations in the total amount of actin present in fibroblasts (Fig. 1D).

To extend these observations to other cellular structures, we investigated the status of focal adhesions and microtubules in those cells lines. The overexpression of c–Myc eliminated the numerous focal adhesions present in RhoA^{Q63L}–transformed NIH3T3 cells (Fig. 2A,B). The negative effect of c–Myc overexpression in the RhoA^{Q63L}–dependent F–actin cytoskeleton was not constitutive, because we observed a restoration of both stress fibers and focal adhesions when cell lines co–expressing RhoA^{Q63L} and c–Myc established extensive cell–to–cell contacts (Fig. 2A,B). The effect of c–Myc in the F–actin cytoskeleton was specific, since it did not have any effect on the microtubule network when overexpressed in either parental or RhoA^{Q63L}–expressing NIH3T3 cells (Supplementary Fig. 1 available online). We have also previously demonstrated that cell lines overexpressing RhoA^{Q63L} and c–Myc are more transforming than those expressing the GTPase alone (Berenjeno et al., 2007). Consistent with the F–actin–specific inhibitory effect of c–Myc overexpression, we observed that the overexpression of c–Myc did not antagonize other RhoA^{Q63L}–mediated responses such as the loss of cell polarity in NIH3T3 cells (Supplementary Fig. 2 available online). These results indicate that the antagonistic function of c–Myc seems to be limited to RhoA–dependent cytoskeletal pathways and cannot be generalized to other unrelated pathways that contribute to cell transformation or cell polarity loss.

c–Myc targets the Rock pathway

Since the formation of stress fibers and focal adhesions by RhoA is regulated by Rock (Amano et al., 1997; Riento & Ridley, 2003), we next investigated the status of this pathway in the presence or absence of overexpressed c–Myc. To this end, we evaluated the phosphorylation levels of two well–known Rock downstream elements, the myosin light

chain (MLC) and the myosin binding subunit of MLC phosphatase (MYPT1) (Fig. 3A) (Amano et al., 1996; Kimura et al., 1996; Riento & Ridley, 2003). In addition, we evaluated MLC, MYPT1, RockI and RockII protein levels in the indicated cells (Fig. 3A). Whereas we did not observe any significant change in the total levels of those four proteins among $RhoA^{Q63L}$– and $RhoA^{Q63L}$/c–Myc expressing cells (Fig. 3B), we found that the phosphorylation levels of both MLC and MYPT1 were severely decreased in cells co–expressing $RhoA^{Q63L}$ and c–Myc (Fig. 3B,C), indicating that c–Myc overexpression leads the inhibition of the Rock pathway in $RhoA^{Q63L}$–transformed cells. Additional experiments indicated that the inhibition of Rock signaling was not due to indirect effects in the membrane localization of $RhoA^{Q63L}$ (data not shown) or to increases in the cytosolic distribution of $p21^{WAF1}$ (Fig. 3D), a cell cycle inhibitor that can bind to Rock and inhibit its catalytic activity (Fig. 3A) (Lee & Helfman, 2004). We could not see either any elevation in the mRNA levels of RhoE (data not shown, but see below, Fig. 5), a GTPase that inactivates Rock (Riento et al., 2003). These results indicate that c–Myc affects negatively the activity of the Rock/MLC pathway in $RhoA^{Q63L}$–transformed cells.

Given the above results, we next investigated whether an increase in the levels of either $RhoA^{Q63L}$ or RockII signals could restore the F–actin cytoskeleton in c–Myc– and $RhoA^{Q63L}$/c–Myc–expressing NIH3T3 cells. To this end, we transiently expressed in cells either an enhanced green fluorescent protein (EGFP) fused to $RhoA^{Q63L}$ or a chimeric protein composed of EGFP, the RockII kinase domain, and the estrogen receptor hormone binding domain (EGFP–RockIIKD–ER protein). The latter protein only becomes activated upon treatment of cells with hydroxytamoxifen (4–OHT) (Croft et al., 2004). The transient expression of EGFP–$RhoA^{Q63L}$ restored stress fibers in both c–Myc– and $RhoA^{Q63L}$/c–Myc–expressing cells (Fig. 4A). Instead, its expression in $RhoA^{Q63L}$–transformed cells did not enhance the numerous stress fibers already present in those cells (data not shown). The EGFP–RockIIKD–ER protein induced the formation of stress fibers in both parental and $RhoA^{Q63L}$–expressing NIH3T3 cells when derepressed by 4–OHT binding (Fig. 4B). The stress fibers induced by the EGFP–RockIIKD–ER chimera showed an aster–like distribution and not the typical parallel network of F–actin fibers, an effect probably derived from the lack of activation of other RhoA downstream elements that contribute to proper stress fiber orientation (i.e., mDia) (Nakano et al., 1999). Similar, radially oriented stress fibers were also induced by the 4–OHT–stimulated EGFP–RockIIKD–ER in $RhoA^{Q63L}$/c–Myc–expressing cells (Fig. 4B). However, in this case the transfected cells spread less efficiently than parental and $RhoA^{Q63L}$–expressing NIH3T3 cells (Fig. 4B). The number of stress fibers per cell induced by the inducible RockII kinase domain was also reduced when compared to those found in the latter cell lines (Fig. 4B). The cytoskeletal effects of the EGFP–RockIIKD–ER chimera were due to its kinase activity, as demonstrated by the lack of stress fiber induction when a catalytically inactive version of this protein was used (Fig. 4B). Taken together, these results suggest that the effect of c–Myc on the F–actin cytoskeleton is probably mediated by two independent routes, one affecting the total signaling output of the RhoA/Rock signaling route (which can be recovered by the overexpression of RhoA or RockII) and another one probably linked to cytoskeletal components related to spreading and focal adhesions that cannot be fully restored by enhanced RhoA/Rock signals.

Characterization of the transcriptomal changes induced by the overexpression of c–Myc in RhoA^{Q63L}–transformed cells

We hypothesized that the negative effects of c–Myc in the F–actin cytoskeleton of RhoA^{Q63L}–transformed fibroblast had to be transcriptome–based. To identify gene targets that could be involved in this response, we carried out Affymetrix microarray analysis using total RNAs obtained from subconfluent cultures of RhoA^{Q63L}–, RhoA^{Q63L}/c–Myc–, and of RhoA^{Q63L}/MadMyc–expressing cells (Berenjeno et al., 2007). Using the selection criteria indicated in the Supplemental Materials and Methods Section, we found a total of 535 genes (239 upregulated, 296 downregulated) whose protein products could be potentially involved in the negative modulation of the RhoA–dependent F–actin cytoskeleton by c–Myc (Fig. 5A and Supplementary Table I available online). Of those 535 genes, 152 genes had opposed expressing profiles between RhoA^{Q63L}/c–Myc– and RhoA^{Q63L}/MadMyc–expressing cells (Fig. 5A and Supplementary Table I). Functional annotation of the proteins encoded by those genes indicated that they were involved in a large variety of cellular functions (Supplementary Table II available online). Most of those proteins did not have any obvious correlation with cytoskeletal regulatory events or cytoskeletal structures. However, we found a small subset of c–Myc targeted loci encoding proteins that could be assigned to three functional categories related to the regulation of cytoskeletal dynamics: (i) Direct upstream regulators of the RhoA pathway. (ii) GTPases that antagonize RhoA signaling routes. (iii) Structural elements of the cell cytoskeleton (Fig. 5B and Supplementary Text available online). Some of those proteins were dismissed since they were unlikely to block signals derived from the constitutively active version of RhoA expressed in the NIH3T3 cell lines used in this study (see Supplementary Text). As a consequence, we decided to focus our attention in the deregulated genes that encoded important cytoskeletal regulators such as Cdc42, Pak1, and integrin subunits (Itgβ1l, Itgβ5 and Itgα5) (Fig. 5B and Supplementary Text). To corroborate the microarray data on those genes, we performed quantitative RT–PCR experiments. As negative controls, we used oligonucleotide pairs to amplify cDNAs encoding integrins (β1, β4) not identified in our arrays. In order to maximize the information gathered from these experiments, we decided to carry out RT–PCR reactions using total RNAs from subconfluent cultures of c–Myc–, RhoA^{Q63L}–, RhoA^{Q63L}/c–Myc– and RhoA^{Q63L}/MadMyc– expressing cells. Using this approach, we wished to verify whether the expression of those genes was dependent exclusively on the expression of c–Myc or, alternatively, on synergistic interactions between the transcriptional programs of c–Myc and RhoA^{Q63L}. These experiments indicated that the *Cdc42* (Fig. 6A) and *Pak1* (Fig. 6B) mRNAs were indeed upregulated in RhoA^{Q63L}/c–Myc–expressing cells when compared to the rest of cell lines used in the study. The upregulation of Pak1 protein in RhoA^{Q63L}/c–Myc–expressing NIH3T3 cells was also demonstrated by immunoblot experiments (Supplementary Figs. 3A and 4A,B). Consistent with the microarray data, we also observed reduced levels of expression for the *Itbl1* (Fig. 6D) and *Itgb5* (Fig. 6E) mRNAs but not for the *Itgb4* transcript (Fig. 6F) in RhoA^{Q63L}/c–Myc–expressing NIH3T3 cells. A significant reduction, not picked up in the microarray experiments, was also observed for the *Itgb1* transcript in that cell line (Fig. 6C). This repression was also observed at the protein level in RhoA^{Q63L}/c–Myc–expressing cells (Supplementary Fig. 3B). Most of the transcript tested were found differentially expressed at statistical significant levels only in RhoA^{Q63L}/c–Myc–expressing cells, indicating that they are regulated by synergistic interactions between

RhoA^{Q63L}–dependent signals and c–Myc. Interestingly, the *Itgb5* mRNA was the only one showing a specific variation in RhoA^{Q63L}/MadMyc–expressing cells, suggesting that it may be one of the key elements promoting the increased numbers in stress fibers observed in this cell line (see above, Fig. 1A,B).

To get an overall view of the synergistic cross–talk among RhoA^{Q63L} and c–Myc at the transcriptional level, we next compared the genes identified as "RhoA^{Q63L}/c–Myc specific" in these experiments with the "RhoA^{Q63L} specific" transcriptome previously described by us in NIH3T3 cells (Berenjeno et al., 2007). Consistent with expression patterns resulting from synergistic interactions between RhoA^{Q63L} signals and overexpressed c–Myc protein, we found that the majority of the deregulated genes present in RhoA^{Q63L}/c–Myc–expressing cells were not present in the transcriptome of RhoA^{Q63L}–expressing fibroblasts (see further details in Supplementary Text). Since our previous results indicated that some of the Rock targets were downmodulated in RhoA^{Q63L}/c–Myc expressing cells (see above, Fig. 3B,C), we also compared the present microarray data with the previously described Rock/Y27632–dependent transcriptome of RhoA^{Q63L}–transformed cells (Berenjeno et al., 2007). We considered that, if c–Myc abrogated all Rock signaling, there had to be a significant overlap between the Rock/Y27632– and RhoA^{Q63L}/c–Myc–dependent transcriptomes. We found that c–Myc overexpression only targeted 4.1% of the 97 Rock/Y27632–dependent genes previously identified as Rock/Y27632–dependent in RhoA^{Q63L}–transformed cells, a result that further suggest that this transcriptional factor does not abolish all Rock–dependent functions in fibroblasts. This is consistent with previous data indicating that c–Myc overexpression, unlike the Y27632 treatments (Berenjeno et al., 2007; Sahai et al., 1999), does not affect RhoA^{Q63L} transforming activity in NIH3T3 cells (Berenjeno et al., 2007). Taken together, these results indicate that the overexpression of c–Myc leads to synergistic interactions with RhoA–dependent signals that result in new patterns of gene expression. Moreover, they suggest that c–Myc overexpression targets the cytoskeletal signaling branch of Rock but not other Rock–related functions.

Increased cell densities overturn the upregulation of Pak1 and integrin subunits found in RhoA^{Q63L}/c–Myc–expressing cells

To further correlate the aforementioned transcriptomal changes with the conditions in which the cell cytoskeleton is inhibited in RhoA^{Q63L}/c–Myc expressing cells, we evaluated the expression of *Cdc42*, *Pak1*, *Itgb1*, *Itbl1* and *Itgb5* genes in dense cell cultures. Quantitative RT–PCR experiments revealed that the expression of *Cdc42* and *Pak1* genes was independent on the density of RhoA^{Q63L}/c–Myc–expressing cells in culture (Fig. 6, panels G and H, respectively). Despite this, we observed that the protein levels of Pak1 were severely diminished in dense cell cultures (Supplementary Fig. 4), suggesting that this kinase may be controlled by a post–transcriptional mechanism upon the establishment of cell–cell contacts. The repression of *Itgb1*, *Itgbl1* and *Itgb5* genes observed in RhoA^{Q63L}/c–Myc–expressing cells was totally eliminated when these cells were cultured at increased densities (Fig. 6, panels I, J and K, respectively). A strong repression of Itgβ1 protein levels in RhoA^{Q63L}/c–Myc expressing cells, which was rescued in high cell density conditions, was also demonstrated using Western blot analysis (Supplementary Fig. 3B). These

experiments indicate that a subset of the RhoA^{Q63L}/c–Myc–dependent transcriptome and proteome can be antagonized by the establishment of cell–to–cell contacts.

Pak1 and integrins contribute to the c–Myc–dependent inhibition of the RhoA–dependent cytoskeleton

We hypothesized that if some of the above genes were involved in the disassembly of stress fibers in RhoA^{Q63L}/c–Myc–expressing cells, the manipulation of the levels of activity and/or expression of their protein products should induce the disruption of the stress fiber network in RhoA^{Q63L}–expressing cells in the absence of c–Myc overexpression or, alternatively, rescue the stress fibers defects in RhoA^{Q63L}/c–Myc–expressing cells. To investigate this possibility, we first analyzed the influence of the Cdc42/Pak1 axis in the stability of stress fibers in RhoA^{Q63L}–expressing NIH3T3 cells. To this end, we infected those cells with retroviruses encoding bicistronically the EGFP and different versions of Cdc42, Rac1, and Pak1 proteins. Those included a fast–cycling mutant (F28L) of Cdc42 that shows constitutive activity in vivo (Lin et al., 1997), a fast–cycling mutant (F28L) of Rac1 (a GTPase that also binds and activates Pak1) (Guo & Zheng, 2004), a Rac1^{F28L} protein containing a point mutation in its switch region (F37A) that eliminates the binding and activation of Pak1 (Joneson et al., 1996), a Rac1^{F28L} protein with a point mutation in the switch region (Y40C) that retains the ability of stimulating Pak1 (Joneson et al., 1996), and the wild type version of Pak1. The expression of Cdc42^{F28L} (Fig. 7A, Supplementary Fig. 5A), Rac1$^{F28L+Y40C}$ (Fig. 7A, Supplementary Fig. 5A) and wild type Pak1 (Fig. 7A,B, Supplementary Fig. 5A,B) led to the disassembly of the F–actin stress fibers in RhoA^{Q63L}–expressing cells. Instead, and consistent with the implication of Pak1 in this process, the expression of the Rac1$^{F28L+F37A}$ mutant had no effects on the cytoskeleton of RhoA^{Q63L}–transformed cells (Fig. 7A, Supplementary Fig. 5A).

To further verify the involvement of Pak1 in the c–Myc–dependent inhibition of the cytoskeleton, we infected RhoA^{Q63L}–, RhoA^{Q63L}/c–Myc– and RhoA^{Q63L}/MadMyc–expressing cells with retrovirus encoding bicistronically the EGFP and a dominant negative Pak1 protein (K298R mutant). The overexpression of that mutant promoted the re–establishment of stress fibers in cells co–expressing RhoA^{Q63L} and c–Myc, indicating that the endogenous Pak1 protein does contribute to the downmodulation of their stress fibers (Fig. 7C, Supplementary Fig. 5C). In agreement with the lack of upregulation of Pak1 in Rho^{Q63L}– and RhoA^{Q63L}/MadMyc–expressing cells, Pak1^{K298R} did not induce any significant effect in the stress fibers of those two cell lines (Fig. 7C, Supplementary Fig. 5C). We observed that the inhibitory effect of Pak1 on the stress fiber network was lost when RhoA^{Q63L}/Pak1–expressing cells established large numbers of cell–to–cell contacts (Fig. 7D, Supplementary Fig. 5D). These experiments indicate that Pak1 overexpression mimics the effects of c–Myc overexpression in the F–actin cytoskeleton of RhoA^{Q63L}–transformed cells.

We next used siRNAs for *Itgb1* and *Itgb5* transcripts to investigate the effects of integrin downmodulation in the stability of stress fibers of RhoA^{Q63L}–expressing NIH3T3 cells. The knockdown of any of these two integrins induced a ≈50% reduction in the total number and thickness of stress fibers (Fig. 7E, Supplementary Fig. 5E). As control, we observed that a

siRNA containing a scrambled nucleotide sequence did not affect the stress fibers present in RhoA^{Q63L}–expressing fibroblasts (Fig. 7E). The knockdown of *Itgb1* and *Itgb5* mRNAs induced loss of adherence and the detachment of cells from the coverslip (data not shown). The knock–down levels of *Itgb1* and *Itgb5* transcripts were verified by RT–PCR experiments (Fig. 7E). Taken together, these results demonstrate that Pak1 and integrin subunits β1 and β5 are integral components of the transcriptional program that eliminates the RhoA/Rock dependent cytoskeleton in RhoA^{Q63L}/c–Myc–transformed NIH3T3 cells.

c–Myc overexpression changes the invasion and adhesion properties of RhoA–transformed cells

To verify whether the RhoA/c–Myc cross–talk had any effect in the biological program of RhoA–transformed cells, we evaluated the invasion and adhesion properties of the cell lines used in this study. We observed that RhoA–transformed cells displayed lower invasive rates than the parental or the c–Myc expressing fibroblasts (Fig. 7F). However, this defective invasiveness was rescued in RhoA^{Q63L}/c–Myc–expressing cells (Fig. 7F). We also observed that RhoA–expressing cells displayed enhanced adhesion to fibronectin, collagen IV, laminin, and fibrinogen when compared to either NIH3T3 or c–Myc expressing cells (Fig. 7G). By contrast, RhoA^{Q63L}/c–Myc–expressing cells show lower levels of adhesion to fibronectin, collagen IV and fibrinogen when compared to RhoA–transformed cells (Fig. 7G). These data indicate that the c–Myc expression status does change at least some of the cytoskeletal–related biological responses mediated by RhoA^{Q63L}.

DISCUSSION

We have unveiled in this work a synergistic cross–talk between RhoA^{Q63L} and c–Myc that, through modification of the cellular transcriptome, promotes the disassembly of stress fibers and focal adhesions in RhoA^{Q63L}–transformed fibroblasts. This cross–talk entails both the upregulation and repression of genes encoding proteins involved in cytoskeletal architecture (i.e., integrin subunits) and regulation (i.e., Cdc42, Pak1) (Fig. 5B). This cross–talk exhibits three remarkable features. The first of them is that the transcriptional regulation of genes involved in this process requires synergistic signals from both RhoA^{Q63L} and c–Myc. A second feature is that c–Myc influences negatively the RhoA/Rock–dependent cytoskeleton while it favors at the same time other RhoA–dependent routes essential for transformation status of RhoA^{Q63L}–expressing cells. This signaling specificity can be applied even within specific branches of the Rock pathway, as inferred from the observations indicating that c–Myc reduces the phosphorylation levels of both MLC and MYPTP1 in RhoA^{Q63L}–transformed cells without compromising the Rock–dependent transcriptome present in those cells. This is probably due to the fact that Pak1 and integrins are located downstream of Rock, a property that ensures the conservation of additional Rock downstream pathways. A third feature of this biological program is that it can be reversed rapidly by intercellular contacts or increased cell densities of cultured cells. Although the elucidation of this counterbalancing pathway remains to be elucidated, our data are consistent with the simultaneous assembly of two different regulatory steps upon the establishment of cell–cell interactions. One of those steps relies on transcriptional–and/or mRNA stability–linked processes, because we have found that the expression levels of *Itgb1*, *Itbl1* and *Itgb5*

transcripts are restored in dense cell cultures. By contrast, another step occurs at the post–transcriptional level since we have observed that increased cell–to–cell contacts affecs negatively the protein levels of Pak1 while they had no effect on its mRNA levels. It is also possible that the establishment of extensive cell contacts could also favor indirectly stress fiber stability by the creation of nucleation sites for the growth of F–actin cables via, for instance, the formation of cadherin/α–catenin complexes at cell junctions.

Although counterintuitive at first sight, the negative regulation of specific downstream branches of the RhoA/Rock pathway by c–Myc may have advantages for the overall tumorigenic program of cancer cells. This is because this route represents a double edge sword for cell motility. On the one hand, it ensures the sequential adhesion and detachment of cells from the cell substrate, a process that favors cell survival, directional migration, motility, invasiveness and extravasation processes. On the other hand, the presence of high levels of RhoA and Rock activity can impair all those processes by favoring excessive and static adhesion of tumor cells to the substrate or, alternatively, by inducing cell rounding and detachment due to excessive F–actin contractility. In this functional scenario, a system that counteracts excessive levels of RhoA and Rock activity will favor the dynamic assembly and disassembly of stress fibers and focal adhesions. However, a system that eliminates permanently the possibility of proper stress fiber and focal adhesion formation will also severely impair cell motility. In this context, it is clear that a regulatory network that ensures a regulatable and selective inhibition of the RhoA/Rock–dependent cytoskeleton will have an obvious advantage to ensure fluid and dynamic F–actin structures and, at the same time, maintain other RhoA–dependent functions that are important for cell growth and tumorigenesis. Consistent with this regulatory model, we have seen that the overexpression of c–Myc does favor a change in the invasion and adhesion properties of RhoA–transformed cells. A foreseeable biological setting where this regulatory system could be highly beneficial for tumor dissemination and metastasis is the case of cancer cell subtypes associated with exacerbated signaling outputs from c–Myc and the RhoA pathway.

Supplementary Material

Refer to Web version on PubMed Central for supplementary material.

ACKNOWLEDGEMENTS

We thank M. Blázquez for technical help. X.R.B. work is supported by grants from the NIH (5R01CA73735), the Spanish Ministry of Science and Innovation (SAF2006–01789, GEN2003–20239–C06–01), the Red Temática de Investigación Cooperativa en Cáncer (RD06/0020/0001), the Castilla y León Autonomous Government (GR97), and the 7th Framework European Union Program (FP7–HEALTH–2007–A–201862). The authors declare that they do not have competing financial interests.

MATERIALS AND METHODS

Cell lines

All NIH3T3 cell lines used in this work have been described previously (Berenjeno et al., 2007). In that reference and the Supplementary Information linked to it online (http://www.nature.com/onc/journal/v26/n29/suppinfo/1210194s1.html?url=/onc/journal/v2 6/n29/

full/1210194a.html), readers can also find information about the proliferative and transforming properties of those cell lines, the culture conditions used, and the expression levels of the proteins ectopically expressed in them. Unless otherwise stated, we used in the experiments of this work cell lines expressing $RhoA^{Q63L}$ (IMB11–1–P cell line), c–Myc (15–2–7 cell line), $RhoA^{Q63L}$ plus c–Myc (16–2–P3 cell line), $RhoA^{Q63L}$ plus MadMyc (12–3–17 cell line) and $RhoA^{Q63L}$ plus a c–*Myc*–specific shRNA (15–6–35 cell line).

Additional information about other methods and reagents can be found in the Supplementary Information available online.

REFERENCES

Amano M, Chihara K, Kimura K, Fukata Y, Nakamura N, Matsuura Y, Kaibuchi K. Science. 1997; 275:1308–11. [PubMed: 9036856]

Amano M, Ito M, Kimura K, Fukata Y, Chihara K, Nakano T, Matsuura Y, Kaibuchi K. J Biol Chem. 1996; 271:20246–9. [PubMed: 8702756]

Berenjeno IM, Nunez F, Bustelo XR. Oncogene. 2007; 26:4295–305. [PubMed: 17213802]

Bos JL, Rehmann H, Wittinghofer A. Cell. 2007; 129:865–77. [PubMed: 17540168]

Bustelo XR, Sauzeau V, Berenjeno IM. Bioessays. 2007; 29:356–70. [PubMed: 17373658]

Croft DR, Sahai E, Mavria G, Li S, Tsai J, Lee WM, Marshall CJ, Olson MF. Cancer Res. 2004; 64:8994–9001. [PubMed: 15604264]

Dransart E, Olofsson B, Cherfils J. Traffic. 2005; 6:957–66. [PubMed: 16190977]

Etienne–Manneville S, Hall A. Nature. 2002; 420:629–35. [PubMed: 12478284]

Guo F, Zheng Y. Oncogene. 2004; 23:5577–85. [PubMed: 15122327]

Hatzoglou A, Ader I, Splingard A, Flanders J, Saade E, Leroy I, Traver S, Aresta S, de Gunzburg J. Mol Biol Cell. 2007; 18:1242–52. [PubMed: 17267693]

Jaffe AB, Hall A. Annu Rev Cell Dev Biol. 2005; 21:247–69. [PubMed: 16212495]

Joneson T, McDonough M, Bar–Sagi D, Van Aelst L. Science. 1996; 274:1374–6. [PubMed: 8910277]

Kimura K, Ito M, Amano M, Chihara K, Fukata Y, Nakafuku M, Yamamori B, Feng J, Nakano T, Okawa K, Iwamatsu A, Kaibuchi K. Science. 1996; 273:245–8. [PubMed: 8662509]

Lee HH, Chang ZF. J Cell Biol. 2008; 181:999–1012. [PubMed: 18559669]

Lee S, Helfman DM. J Biol Chem. 2004; 279:1885–91. [PubMed: 14559914]

Lin R, Bagrodia S, Cerione R, Manor D. Curr Biol. 1997; 7:794–7. [PubMed: 9368762]

Mueller BK, Mack H, Teusch N. Nat Rev Drug Discov. 2005; 4:387–98. [PubMed: 15864268]

Nakano K, Takaishi K, Kodama A, Mammoto A, Shiozaki H, Monden M, Takai Y. Mol Biol Cell. 1999; 10:2481–91. [PubMed: 10436006]

Olofsson B. Cell Signal. 1999; 11:545–54. [PubMed: 10433515]

Ongusaha PP, Kim HG, Boswell SA, Ridley AJ, Der CJ, Dotto GP, Kim YB, Aaronson SA, Lee SW. Curr Biol. 2006; 16:2466–72. [PubMed: 17174923]

Park SY, Lee JH, Ha M, Nam JW, Kim VN. Nat Struct Mol Biol. 2009; 16:23–9. [PubMed: 19079265]

Riento K, Guasch RM, Garg R, Jin B, Ridley AJ. Mol Cell Biol. 2003; 23:4219–29. [PubMed: 12773565]

Riento K, Ridley AJ. Nat. Rev. Cell Biol. 2003; 4:446–456.

Sahai E, Garcia–Medina R, Pouyssegur J, Vial E. J Cell Biol. 2007; 176:35–42. [PubMed: 17190792]

Sahai E, Ishizaki T, Narumiya S, Treisman R. Curr Biol. 1999; 9:136–45. [PubMed: 10021386]

Shiio Y, Donohoe S, Yi EC, Goodlett DR, Aebersold R, Eisenman RN. Embo J. 2002; 21:5088–96. [PubMed: 12356725]

Wang HR, Ogunjimi AA, Zhang Y, Ozdamar B, Bose R, Wrana JL. Methods Enzymol. 2006; 406:437–47. [PubMed: 16472676]

Wang HR, Zhang Y, Ozdamar B, Ogunjimi AA, Alexandrova E, Thomsen GH, Wrana JL. Science. 2003; 302:1775–9. [PubMed: 14657501]

Ward Y, Yap SF, Ravichandran V, Matsumura F, Ito M, Spinelli B, Kelly K. J Cell Biol. 2002; 157:291–302. [PubMed: 11956230]

Watnick RS, Cheng YN, Rangarajan A, Ince TA, Weinberg RA. Cancer Cell. 2003; 3:219–31. [PubMed: 12676581]

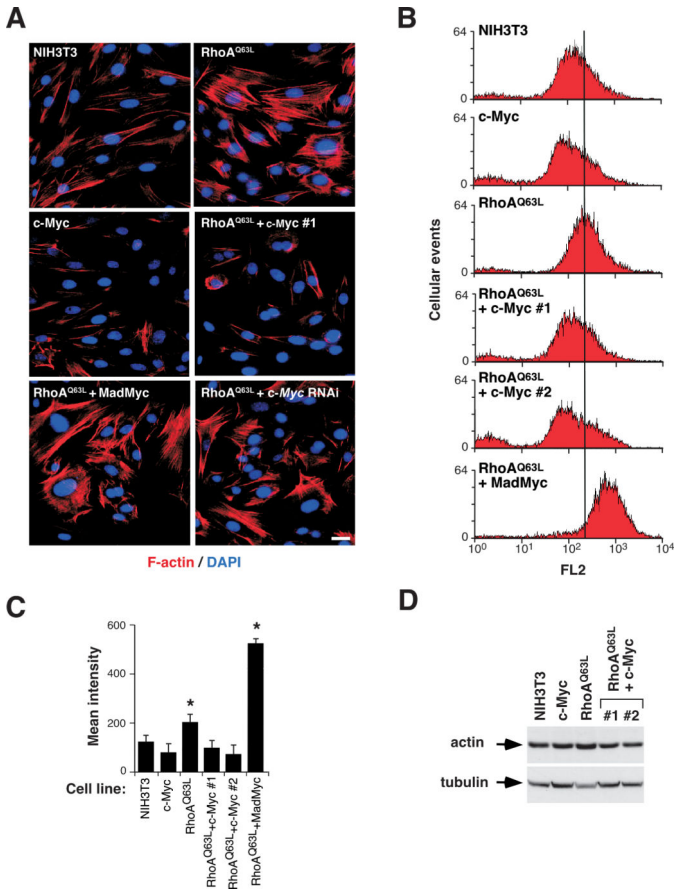

FIGURE 1.

c–Myc induces a reduction of stress fibers in rodent fibroblasts. **(A)** NIH3T3 cells expressing the indicated molecules were fixed and stained with rhodamine–labeled phalloidin and 4',6–diamidino–2–phenylindole (DAPI) to visualize the F–actin cytoskeleton and nuclei, respectively. After staining, cells were analyzed by confocal microscopy. Signals from F–actin and DAPI are shown in red and blue color, respectively. Scale bar, 20 μm. **(B,C)** Flow cytometry analysis (**B**) and quantitation (**C**) of the F–actin levels present in the indicated cell lines ($n = 3$). *, $P \leq 0.01$ compared to parental NIH3T3 cells. **(D)** Expression levels of actin (top panel) and β–tubulin (bottom panel) in total cellular extracts derived from the indicated cells (top). In **A–D**, RhoA^{Q63L}+c–Myc #1 and #2 refer to the IMB11–1–P and IMB11–2P cell lines, respectively.

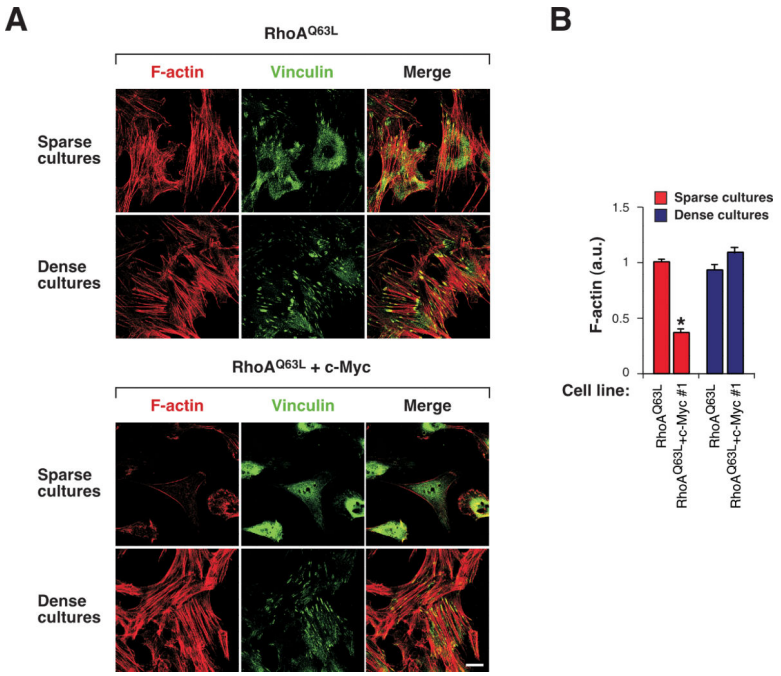

FIGURE 2.

The loss of stress fibers in RhoA^{Q63L}/c–Myc–expressing NIH3T3 cells is rescued by cell–to–cell contacts. **(A)** NIH3T3 cells expressing the indicated ectopic proteins (top) and derived from the indicated culture conditions (left) were stained with rhodamine–labeled phalloidin and incubated with antibodies to vinculin to visualize F–actin fibers and focal adhesions, respectively. Signals from F–actin and vinculin are seen in red (left columns) and green (middle columns), respectively. Areas of co–localization between these proteins are seen in yellow (right columns). Scale bar, 20 μm. **(B)** Quantitation of F– actin levels in the indicated cell lines and culture conditions. *, $P \leq 0.01$ compared to parental NIH3T3 cells. a.u., arbitrary units.

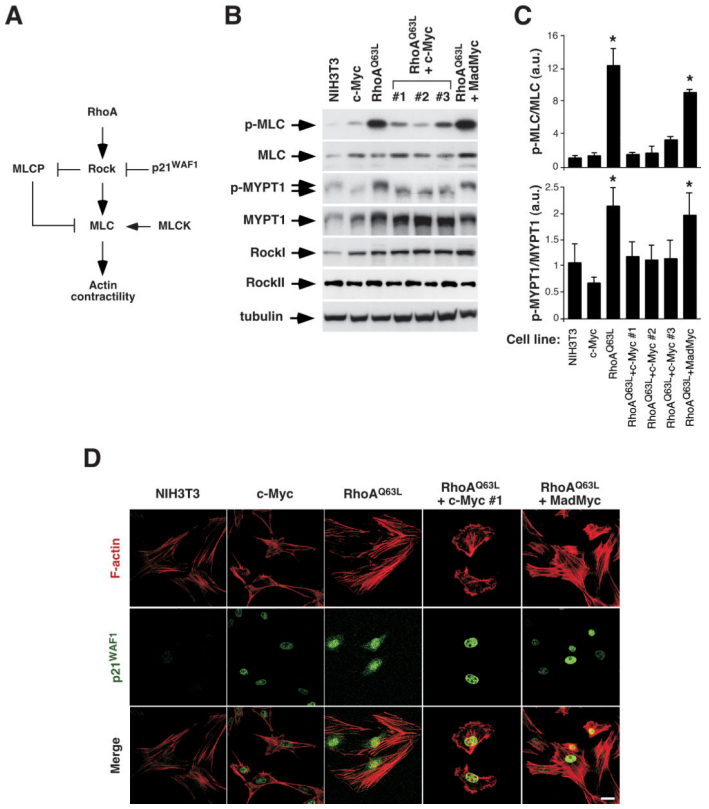

FIGURE 3.

c–Myc targets the Rock pathway in RhoA^{Q63L}–transformed cells. **(A)** Schematic representation of the RhoA/Rock pathway leading to actin contractility. **(B)** Immunoblot analysis showing the protein expression and/or phosphorylation levels of the indicated proteins (left) in the cell lines used in this study (top). p–, phosphorylated. RhoA^{Q63L}+c–Myc #1, #2 and #3 refer to the IMB11–1–P, IMB11–2P and IMB11–3P cell lines, respectively. **(C)** Quantitation of phosphorylation levels of MLC (top panel) and PYPT1 (lower panel) obtained in three independent experiments. *, $P \leq 0.01$ compared to parental NIH3T3 cells. **(D)** Subcellular localization of p21^{WAF1} in the indicated cell lines (top). Fluorescence signals derived from phalloidin–stained F–actin and the p21^{WAF1} antibodies are shown in red (upper row of panels) and green (middle row of panels), respectively. Areas of co–localization had to be seen in yellow if present (bottom row of panels). Observe that RhoA^{Q63L}/c–Myc expressing cells, unlike the case of RhoA^{Q63L}–transformed cells, do not show any cytoplasmic staining of p21^{WAF1}. Scale bar, 20 μm.

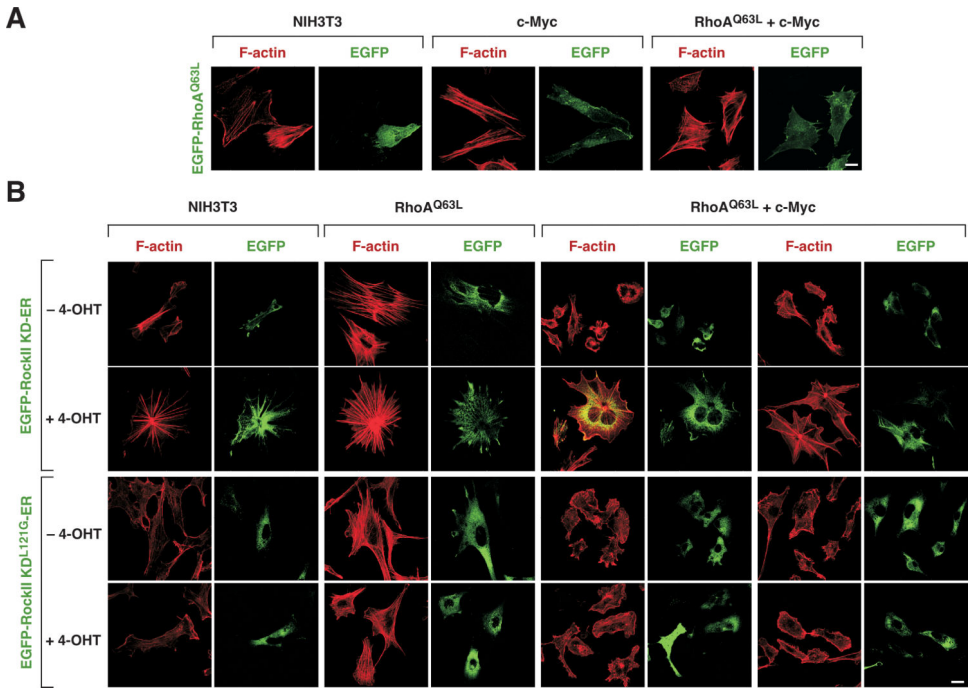

FIGURE 4.

Expression of RhoA^{Q63L} or the RockII kinase domain partially rescues the stress fiber defects present in RhoA^{Q63L}/c–Myc–expressing NIH3T3 cells. **(A,B)** Cell lines expressing the indicated proteins (top) were either transfected with a mammalian expression vector encoding EGFP–RhoA^{Q63L} (**A**) or infected with retroviruses expressing either an active (**B**) or a catalytically inactive (L121G mutant) (**B**) version of the EGFP–RockIIKD–ER protein. In the case of panel **B**, cells were either left untreated (–4–OHT) or treated (+4–OHT) with 4–OHT after the transfection, fixed, and analyzed by microscopy. Signals from EGFP fusion proteins and F–actin are seen in red and green, respectively. Scale bars, 10 (**A**) and 20 (**B**) μm.

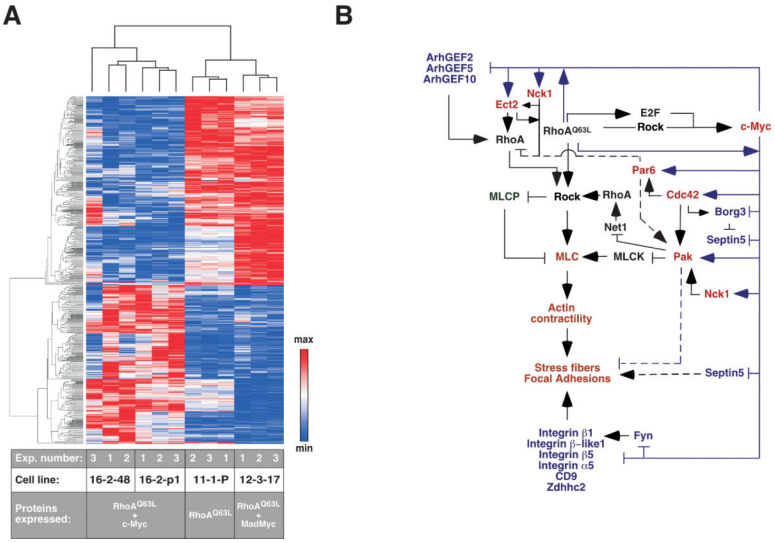

FIGURE 5.

Characterization of the transcriptomal changes present in RhoA^{Q63L}/c–Myc–expressing cells. **(A)** Hierarchical cluster diagram of the 535 genes whose expression level changed in RhoA^{Q63L}/MadMyc– or RhoA^{Q63L}/MadMyc–expressing proteins relative to the transcriptome of RhoA^{Q63L}–transformed NIH3T3 cells. Each column represents one experiment and each row a gene. Varying levels of expression are represented on a scale from dark blue (lowest expression) to dark red (highest expression). Note that expression values are represented as signal log ratio numbers and that, therefore, the total fold change value is obtained from 2^{SLR}. The experiment number, the cell line and the proteins expressed in the indicated cell lines are indicated at the bottom. **(B)** Schematic representation of the molecular network that can potentially interfere with RhoA signaling, stress fibers and focal adhesions in RhoA^{Q63L}/c–Myc–expressing cells. Transcriptionally–regulated gene products are color–coded in red (upregulated) or blue (downregulated). Known connections among signal transduction elements are indicated with black lanes. Connections revealed in the present work are indicated with blue lanes. Discontinuous lanes indicate pathways involving the participation of other signaling elements that had not been depicted in the figure. In addition, we have also highlighted in green color proteins with increased catalytic activity according to immunoblots analysis (see Fig. 3B,C). We have also pin–pointed in brown color proteins and cellular structures that, according to Figs. 1–3, show decreased activity or levels in RhoA^{Q63L}/c–Myc–expressing cells. The participation of the transcriptional factor E2F and Rock in the activation of the endogenous *c–Myc* locus has been shown before (Berenjeno et al., 2007). For the participation of c– Myc and RhoA^{Q63L}–derived signals in the activation of the indicated genes, see further experiments presented in this work (see main text, **Fig. 5** and Supplementary Figure 3).

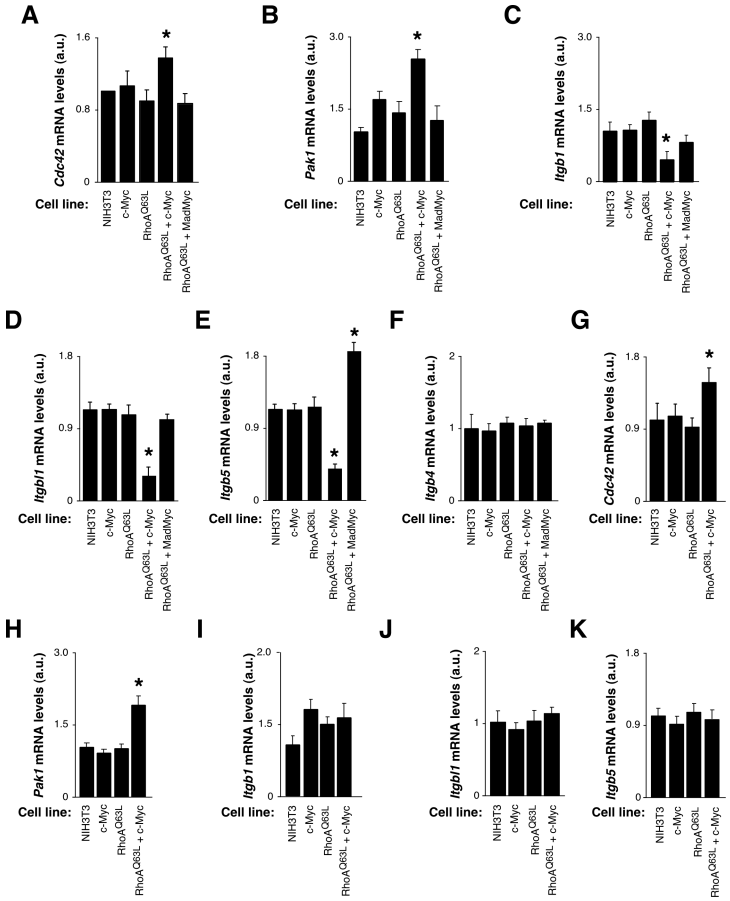

FIGURE 6.

Corroboration of the molecular networks identified in Fig. 5B by quantitative RT–PCR. **(A–K)** Relative expression levels of *Cdc42* (**A,G**), *Pak1* (**B,H**), *Itgb1* (**C,I**), *Itbl1* (**D,J**), *Itgb5* (**E,K**), and *Itgb4* (**F**) transcripts in the indicated cell lines (bottom) that were harvested under low (**A–F**) and high density (**G–K**) culture conditions. Values are expressed as fold–change of the appropriate mRNA respect to the transcript levels found in parental NIH3T3 cells (n = 3). *, $P \leq 0.01$ compared to parental NIH3T3 cells.

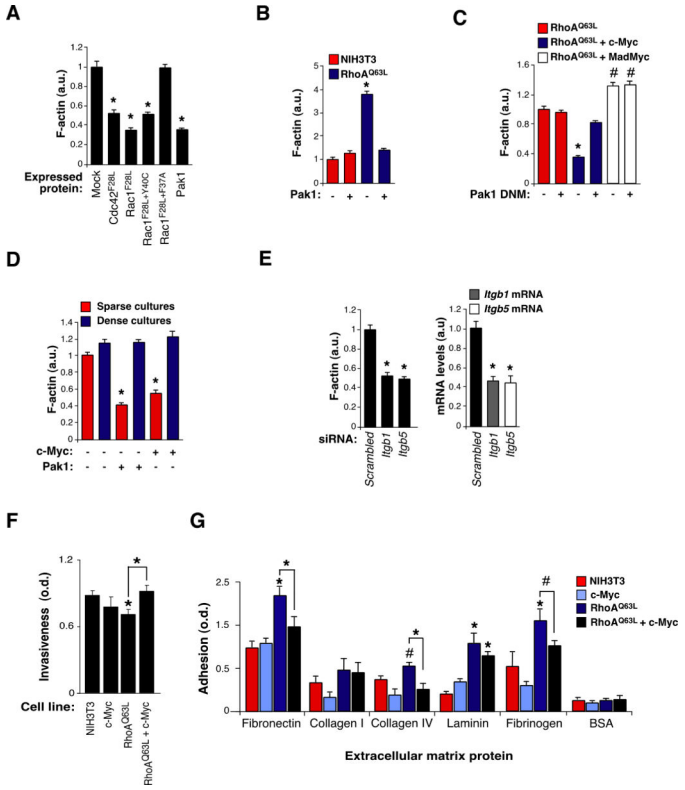

FIGURE 7.

Pak1 and integrin β subunits are involved in the disruption of stress fibers in RhoA^{Q63L}/c–Myc–expressing fibroblasts. **(A)** RhoA^{Q63L}–transformed cells were infected with retroviral particles encoding the indicated proteins (bottom) and the levels of F–actin fibers determined (n = 3). *, $P \leq 0.01$ compared to mock–infected cells. **(B,C)** Effect of the overexpression of wild type Pak1 (**B**) and a dominant negative mutant (DNM) of Pak1 (**C**) in the F–actin cytoskeleton in the indicated cell types (inset) (n = 3). #, $P \leq 0.05$; *, $P \leq 0.01$ compared to either mock–infected NIH3T3 (**B**) or mock–infected RhoA^{Q63L}/c–Myc–expressing (**C**) cells. **(D)** RhoA–transformed (–) or RhoA^{Q63L}/c–Myc expressing (c–Myc+) cells were infected with retrovirus encoding bicistronically wild type Pak1 and EGFP (+) or, alternatively, with retroviruses containing only EGFP (–). At the indicated cell density levels (insets), cells were fixed and F–actin levels quantified (n = 3). *, $P \leq 0.01$ compared to mock–infected RhoA–transformed cells. **(E)** RhoA^{Q63L}–transformed NIH3T3 cells were transfected with the indicated siRNAs (bottom) and, 48 h later, the levels of stress fibers (left panel) and integrin–encoding transcripts (right panel) were evaluated by confocal microscopy and RT–PCR, respectively (n = 3). *, $P \leq 0.01$ compared to RhoA–transformed cells transfected with the control siRNA. **(F)** The invasiveness of the indicated cells lines (bottom) was determined as indicated in the Supplementary Materials and Methods (n = 3, each performed in triplicate). *, $P \leq 0.01$ compared to either parental NIH3T3 cells or the indicated experimental subsets (brackets). **(G)** NIH3T3, c–Myc–, RhoA^{Q63L}– and RhoA^{Q63L}/c–Myc–expressing cells (insets) were subjected to adhesion assays with the indicated extracellular matrix proteins and control bovine serum albumin (BSA) (bottom) (n

= 3, each performed in quadruplicate). #, $P \leq 0.05$; *, $P \leq 0.01$ compared to either parental NIH3T3 cells or the indicated experimental pairs (brackets). o.d., optical density.